
Article:
Watson, M., Fois, N. and Marshall, M.B. (2015) Effects of blade surface treatments in tip – shroud abradable contacts. Wear. ISSN 1873-2577

https://doi.org/10.1016/j.wear.2015.06.018

Effects of blade surface treatments in tip – shroud abradable contacts

M. Watson, N. Fois, M.B. Marshall*

Department of Mechanical Engineering, The University of Sheffield, Mappin Street, Sheffield S1 3JD, UK

* Corresponding author.
Michael Watson
The University of Sheffield,
Mappin Street,
Sheffield S1 3JD,
UK
E-mail address: mea08mw@sheffield.ac.uk
Tel.:+447794920847

Abstract

In aero engines a thermally sprayed abradable lining is applied to the inside of the casing in order to provide a seal around the tips of the compressor blades. As engines become more efficient the materials used must be able to endure higher temperatures and moving parts must be made lighter. This combination is not currently possible in late stages of the compressor as hard abradable materials can cause titanium blades to wear excessively. One solution to this is to add a surface treatment to the blade tips.

Two surface treatments have been investigated, firstly cubic boron nitride (cBN) grits are bonded to the tip of the blade by electroplating. Secondly blades are coated in Cr(Al)N by cathodic arc deposition. The performance of these surface treatments is investigated on a test rig capable of monitoring the blade length, rub forces and abradable temperature during the test. Additional tests are performed against stepped coatings giving insight into the condition of the blade and abradable during the test. S.E.M., E.D.S., X.R.F., profilometry and wear debris have been used to characterise the wear mechanisms produced during the tests.

Grit (cBN) tipped blades load with abradable material after a period of efficient cutting causing grit pull out and fracture. Flat Cr(Al)N coated blades failed due to thermal damage to the coating caused by adhesion of abradable material onto the Cr(Al)N coating, while chamfered blades cut efficiently at low incursion rates.

Key words: Thermal spray coatings, Wear testing, Other surface engineering processes, Ultra-hard materials

1. Introduction

Abradable materials are composite materials which are often used to maintain air seals in aero engines and other turbo machinery[1]–[3]. When used in aero engine compressors they should wear in preference to the blades that contact them with low forces in the rub, leaving smooth surfaces to reduce drag. However they must not degrade in the heat and pressure of the engine or erode excessively if the engine ingests water for example[4]. This combination of properties is normally pursued by thermally spraying a composite lining material which consists of a metal matrix and a non-metal dislocator phase along with some porosity[5]. However ex-service components and numerous experimental studies have shown the potential for excessive blade wear[1]–[3].

Works on abradable materials largely fall into four categories, firstly much work has been done on characterising these materials in laboratory tests. Methods for the measurement of bulk mechanical properties[6]–[8], erosion resistance[9] and abradability[10] have been suggested and form an important measure used in the development of new abradable materials. Experimental investigations have used scaled test platforms to test these materials in situations similar to those they will face in service, these tests typically cover a variety of blade speeds and rates of incursion of the blade into the abradable lining. Other works have attempted to thermally model the rub using bulk properties for the materials, these models are normally validated using data from a test platform[11]. Lastly some attempts have been made to model the microstructure of the abradable materials using an image based finite element approach although these works are largely unverified by experimental findings[12], [13].

Xiao and Matthews[10] compared results from simple scratch tests with those from a full scale test rig and concluded that these results showed good agreement. However more recent tests[1] and models[11] have indicated the importance of heat generation and dissipation during continuously

rubbing systems, additionally further characterisation of rubs has shown significant variation of behaviours at different incursion rates and to a lesser extent blade speeds[3], [2]. Due to their porosity it has also been found that the properties of these materials can locally change during the rub due to compaction[1], [14].

Further experiments on test rigs have focused on characterising rubs either by examining a small number of rubs or attempting to obtain steady state conditions during a test which includes hundreds or thousands of individual rubs. Padova et al[15], [16] investigated rubs with a spin pit facility capable of measuring forces during a single strike concluding that the abradable linings have the greatest effect when the blade is rubbing within the initial surface roughness produced during the thermal spray procedure, they also noted the possibility of low blade speeds allowing for axial deformation of the blades during the rub due to the loss of stiffness produced by high centrifugal forces.

Taylor et al[14] investigated the In-718 vs NiCrAl-Bentonite rub, which is the subject of this work, on an experimental rig capable of recreating the speeds found in in-service engines. Each test consisted of hundreds of individual rubs and the forces in the rub were measured with a dynamometer attached to the abradable sample. They observed significant blade wear in rubs where the abradable had become compacted and lost some of its initial porosity near the rubbing surface. The changes in material properties found by Taylor et. al.[14] for this abradable material and high temperatures measured in previous scaled test rig experiments[1] suggest that a scaled test platform is the most accurate means of assessment of new material combinations in this case.

The potential for research into these interactions is vast due to the many different types of abradable materials available and the variation possible within each by manipulation of the spraying process parameters. Crucially experimental tests that have found compaction in the abradable materials indicate that these materials may not be directly comparable and a single rubbing mechanism is unlikely to be found that can generally describe all of the possible interactions[1], [14].

As aero engines are pushed for higher efficiency and lower weight losses associated with blade wear are of increasing importance. With the current move to single piece bladed disks surface treatments at the blade tip could also allow lighter materials to be used without the risk of blade wear or titanium fires. As an attempt to limit the potential for damage to the blades, this work will investigate the effect of the addition of two different surface treatments to the tip of the blade. Firstly abrasive grains of cBN have been added the effects of changes in size and type of grain have been investigated. Secondly a thin hard coating of Cr(Al)N has been added and the effect of changing the shape of the blade tip has been investigated.

2. Methodology

2.1 Abradables

The tests presented in this work were performed with NiCrAl-Bentonite clad coating samples, these were rubbed against Inconel 718 blade samples. The coating is produced by flame spraying a powder consisting of roughly spherical 120-135µ diameter bentonite particles which have been chemically clad with a thin layer of NiCrAl (Ni 4Cr 4Al)[17] this powder is commercially available as Sultzer Metco 314. The coating has been sprayed in a 60mm square patch onto 80mm square stainless steel backing plates as shown in figure 1a. Before testing the coatings were aged in air at 750^{o}c for 100 hours. A polished cross section of the abradable material used was obtained using vacuum impregnation (buehler epothin 2), further coating sections, discussed below, have been obtained

using the same method. The image obtained by backscattered electrons is shown in figure 1b, S.E.M. was used to limit the effect of crack opening during metallographic preparation[18]. Eight adjacent backscattered micrographs were taken across the entire sample, these were analysed by automatic selection of two threshold values based on the image histogram[19] this method was adapted from Deshpande et. al.[18]. The results of the image analysis indicated the coating is composed of 32.3%vol (stdev=1.77%) porosity, 29.0% (stdev=0.97%) bentonite and 38.7% (stdev=1.06%) metal phase. Variations in coating structure and composition can be introduced by the flame spraying process, because of this, coating samples used were sprayed in a single batch. The mean superficial hardness of these coating samples as given by the R15Y scale is 23.1 with a standard deviation of 9.3 across 100 measurements taken on 10 different samples. The hardness values of the coating samples were compared using a single factor ANOVA the result was not significant f(1.98)=1.40 indicating that there is not significant variation between the coating samples.

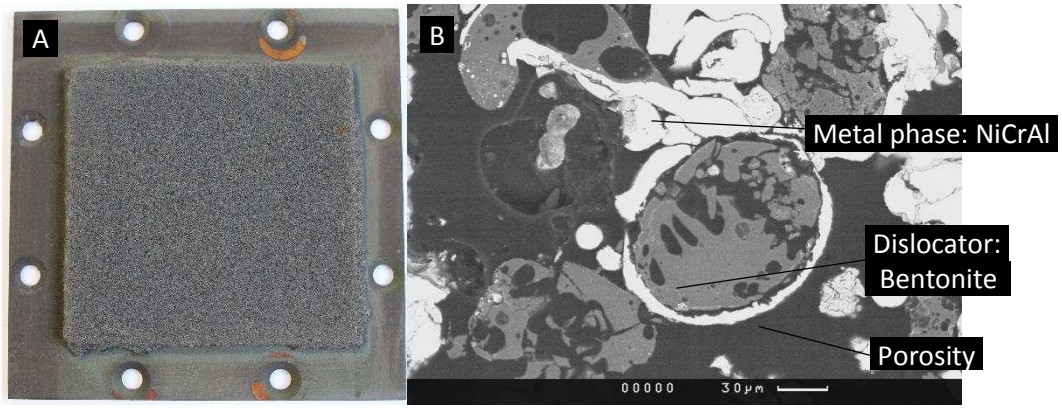

Figure 1 a,b showing a coating sample before testing and a backscattered electron image of the abradable lining material's microstructure.

2.2 Blade surface treatments

Blade specimens have been cut from 2mm thick Inconel 718 which had been vacuum heat treated for 8 hours at 700°c. The blade specimens are 20mm wide and 25mm long with a shape shown in figure 2a. These blades were prepared with two different surface treatments and are contrasted to a control set which had no surface treatment. Two sets of blades were coated with a multilayer Cr(Al)N coating using cathodic arc deposition, a coating of thickness 9.6µm was measured with a micro hardness of 24GPa the appearance of this coating is shown below in figure 2g. One set of these blades was prepared with a flat tip while another set was given a 30° chamfer on the tip to resemble a cutting tool, these are shown in figures 2e and 2f respectively.

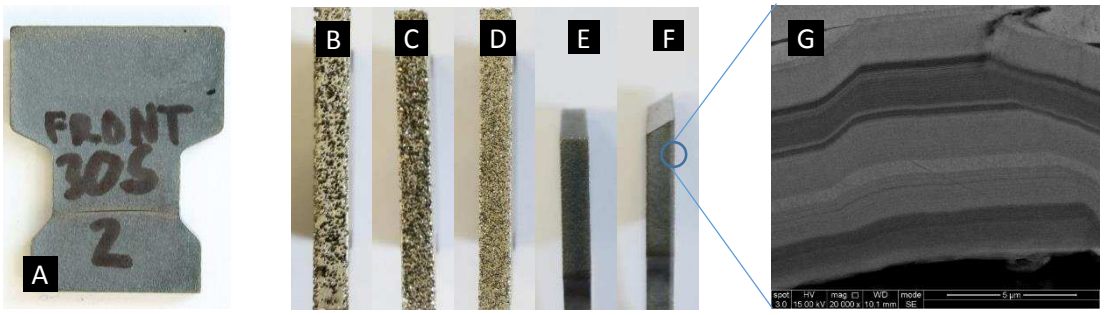

Figure 2 (a-g) showing the shape of the blade samples, tips of blades prepared with large, medium and small grits, the flat and chamfered tip morphologies of the Cr(Al)N blades used and a secondary electron image of the Cr(Al)N coating, with the Inconel 718 substrate the top of the image respectively. Blades are 20mm wide and 2mm thick.

Further sets of blades were tipped with a coating of electrolytically deposited nickel partially covering grains of cBN. This was created by first holding the samples in a PTFE mixture before masking off the entire blade apart from the tip using Kwiky-mask (Greentree Engineered Masking Solutions, Gloucestershire, U.K.). The blades were then submerged in a solution of nickel sulphamate (Nickel Sulphamate MS schloetter) with suspended grains of cBN. The solution was agitated throughout the process by a reciprocating plate. A soluble nickel cathode was used to refresh Ni^{+} ions in the solution and the time allowed for deposition was adjusted to give a depth equal to 40% of the grit size for each grit type. Five different grit types, detailed in table 1, were used exploring the effect of changing both size and type of the grits. cBN grits were provided by Element six, small medium and large high strength grits were used from the 800 series of grit which display a predominantly truncated tetrahedral morphology, additionally a low strength grit (300 series) which have traditionally been used in single layer electroplated tooling were also used. Figure 2b-c shows the appearance of the tips after electroplating.

Set number	Grit type	Grit size	Grit size (µm)	Plating time (min)
8S	800	200/230	66-74	40
8M	800	100/120	125-149	80
8L	800	60/80	177-231	135
3M	300	100/120	125-149	80

Table 1 grit types and sizes used in testing

2.3 Testing

Tests were performed using a bespoke test platform which has previously been described in detail[2], [20], [1] and has successfully reproduced wear mechanisms similar to those observed in an aero engine. The test rig is based around a bench mounted machine tool spindle with a maximum operating speed of 21,000 rpm. A disk capable of holding 2 blades at 180° (radius = 92.5mm) is mounted to the spindle. For each test a single active blade is loaded into the disk with a shorter dummy blade also loaded for balance as shown in figure 3. The incursion rate of the coating is controlled by a z axis microscope stage mounted below the disk which can be controlled between 0.1 and 2000µm/s with an interval of 0.1µm/s. During the test this is used to raise a coating specimen into the path of the blade, the incursion is controlled by a LabVIEW (National instruments 2012) program which also collects and saves data from the sensors described below. Throughout this work incursion rate is discussed in terms of the depth of cut of the blade per pass.

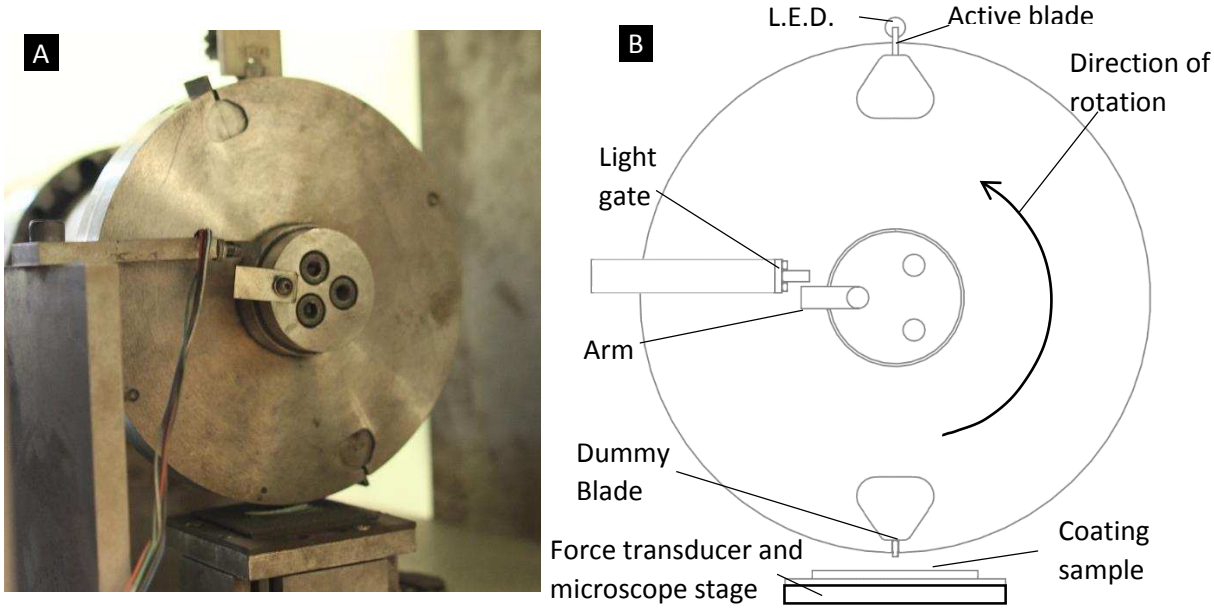

Figure 3 a,b showing a schematic drawing of the test rig and an image of the rig after a test respectively.

The platform uses stroboscopic imaging to monitor the active blade throughout the test. An LED is triggered by an arm on the disk passing through a light gate and controlled by a strobe controller. It is placed directly in front of the camera and timed to flash when the blade is between the LED and the camera, this produces a silhouette of the blade which is captured by the camera. Images from the high speed camera are later analysed in MatLab (mathworks 2013a) to give blade length change from the start of the test. This method is used to measure blade length to an accuracy of ±0.012mm and gives a continuous monitor of the blade length throughout the test.

Force measurements are collected using a piezoelectric force transducer (Kistler Instruments Ltd, Hook, (UK), Type 9347 C) which is capable of measuring both the normal and tangential force of each strike with a sampling frequency of 100kHz (tangential force range: -5kN to 5kN, normal force range: -30 kN to 30 kN, with natural frequencies of 3.6 kHz and 10 kHz respectively for the tangential and normal axes). The force measurement system has been calibrated prior to testing and the dynamic aspects of the test platform have previously been investigated[1] leading to the conclusion that indicative force results are recorded without the need for compensation of the signal. The ratio of these forces can aid identification of changes in the wear mechanism, this is calculated as the tangential force divided by the normal force of the strike.

An infra-red contactless pyrometer (Micro–epsilon, Koenigbacher, Germany) with a threshold temperature of 150°c and a maximum measuring temperature of 1000°c is used to measure the temperature of the centre of the abradable coating sample with a frequency of 25Hz. Further details of the measurement techniques can be found in previous papers[2], [20], [1].

These results are plotted against the total rub length of the blade, this is found using equation 1. In some cases the blade is heavily worn across its entire width in these cases the blade length data are used to calculate the actual rub length of the shorter blade, by treating the disk radius as a function of the pass number.

$$L(P) = \sum_{p=1}^{P} 2R(p)\cos^{-1}\left(\frac{R(p) - Ip}{R(p)}\right)$$

Equation 1

Where $L(P)$ is the rub length as a function of the number of passes, this can be related back to time using the test speed. $R(p)$ is the radius of the disk, p is the pass number and I is the incursion rate of the test in m/pass.

2.4 Post-tests analysis

Where necessary transfer to or from coatings has been identified using a fiscerscope XAN 250 X-ray fluorescence measuring instrument using a 2mm aperture with 50kV electrons passed through a nickel filter, the measurement time for each measurement was 60 seconds. Due to the variability present in thermally sprayed coatings 50 measurements have been taken of the coating in its as sprayed condition as a control group against which comparisons can be made. The Nickel, Chromium and Aluminium contents of the small sampled area vary greatly between measurements, however iron is present as an impurity in both the bentonite clay and the metallic phase at a mean of 0.917% with a standard deviation of 0.153% this is used to identify transfer of Inconel 718 (minimum 11% iron). The ratio of chromium to nickel is also constant as these elements are only present in the

metallic phase, Cr%/Ni% mean is 0.0758 with a standard deviation of 0.00721, this has been used where applicable to identify transfer of the Cr(Al)N coating.

3. Results

The blades in this study were tested at 200m/s tip speed with incursion rates of 2 and 0.02 µm/pass, 200m/s and 0.02 µm/pass has been shown to accurately represent wear mechanisms found in flight[2] whereas 200m/s 2µm/pass is intended to represent incursions during engine commissioning. A list of the tests performed is shown in table 2 as well as a naming convention which is used throughout this work.

Test No.	Blade Type	Sub type	Grit size	Incursion rate µm/pass
1-NO1	No treatment	-	-	0.02
2-8S1	Grit tipped	800	Small (66-74µm)	0.02
3-8M1	Grit tipped	800	Medium (125-149µm)	0.02
4-8L1	Grit tipped	800	Large (177-231µm)	0.02
5-3M1	Grit tipped	300	Medium (125-149µm)	0.02
6-CF1	Cr(Al)N Coating	Flat	-	0.02
7-CC1	Cr(Al)N Coating	30° chamfer	-	0.02
8-NO2	No treatment	-	-	2
9-8S2	Grit tipped	800	Small (66-74µm)	2
10-8M2	Grit tipped	800	Medium (125-149µm)	2
11-8L2	Grit tipped	800	Large (177-231µm)	2
12-3M2	Grit tipped	300	Medium (125-149µm)	2
13-CF2	Cr(Al)N Coating	Flat	-	2
14-CC2	Cr(Al)N Coating	30° chamfer	-	2

Table 2 List of tests completed

3.1 Control tests - plain Inconel blade

The recorded normal force, coating temperature and change in blade length for the untreated blade at 0.02µm/pass are shown in figure 4a. The coating is cleanly cut with no blade wear observed during the test and wear only present on a small portion of the blade during post-test examination. The surface of the coating shows a large, rough wear track as is characteristic of a clean cutting mechanism, with the abradable dislocating as intended. X-ray fluorescence determined the composition of the wear track is within the expected range for the abradable coating, indicating that no measurable transfer has occurred.

A	0.02µm/pass	B	2µm/pass

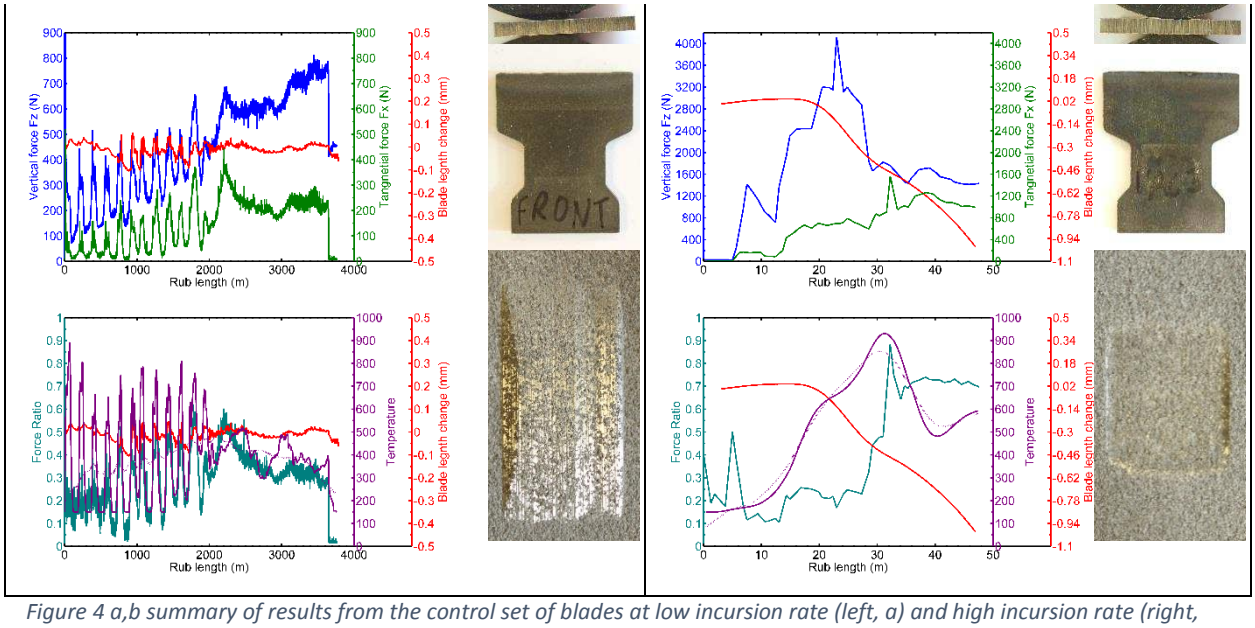

Figure 4 a,b summary of results from the control set of blades at low incursion rate (left, a) and high incursion rate (right, b). Blades and rub tracks are 20mm wide, blades are 2mm thick.

Early in the test cyclic behaviour is observed in the normal force, tangential force, measured blade length and temperature with a period of around 14 seconds or 350 strikes. Examination of single cycles of this behaviour shows the force increases initially followed by temperature, this is shown in figure 6 below. This order is indicative of blade growth on contact artificially increasing the incursion rate causing an increase in force. In the case of adhesions or thermal expansion of the blade this growth is unstable and the shrinking of the blade either by loss of adhered material or cooling results in much lower incursion rates or loss of contact between the peaks shown in figure 6. The slow drop off of forces at the end of the force peak in this case is indicative of behaviour driven by thermal expansion.

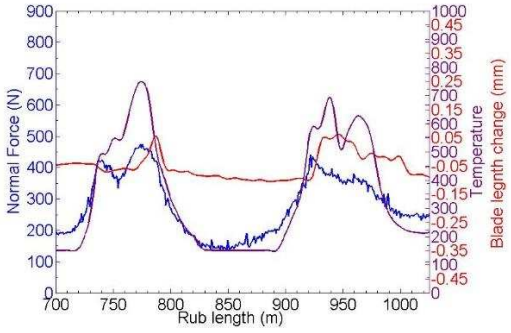

Figure 5 showing single cycles of the cyclic behaviour observed in low incursion rate tests.

At 2µm/pass the normal force and temperature increase early in the test. At this point the blade wears preferentially to the coating and there is a large loss of blade length during the test as shown in figure 4b. The blade tip is slightly grooved while the coating appears rough and dull, similar to the as sprayed state. X-ray fluoresce indicated there had been transfer of the blade material on to the coating at the edges of the wear track (1.71% Fe, 5.2 standard deviations above mean), transfer could not be identified in the centre of the track (1.06% Fe, 0.936 standard deviations above mean) indicating that the blade material has been removed in chips and not by adhesive transfer. The change in preference of worn material from abradable lining to blade has previously been observed[3], [1], [21] and modelled for similar rubs using finite difference modelling[11]. It is

thought to be a result of very high temperatures causing softening of the blade material[11] leading to it shearing in thin planes[14]. The presence of large shear lips on the trailing edge of the blade[14] and measurements of high temperatures during the test suggest that this mechanism is dominant in this case.

3.2 Low incursion rate (0.02µm/pass)

3.2.1 Grit (cBN) tipped blades

The grit tipped blades with the exception of the largest grit (4-8L1) are worn flat with no grits visible on the surface, all of the wear tracks on the coating samples appeared cleanly cut with a shiny surface, similar to those produced by an untipped blade, this is shown in figures 6a and b. XRF analysis of the coating could not confirm the shiny layer as adhesive transfer for any of the tests. The tips of the worn blades were imaged with S.E.M. this showed small fragments of grits remained on the blades from tests 5-3M1 (50µm max size) and 3-8M1 (100µm) as shown in figure 6c. The large grits on the blade from test 4-8L1 appeared intact, however S.E.M. imaging (figure 6d) shows there has been significant pull out of cBN and some loading onto the remaining grains.

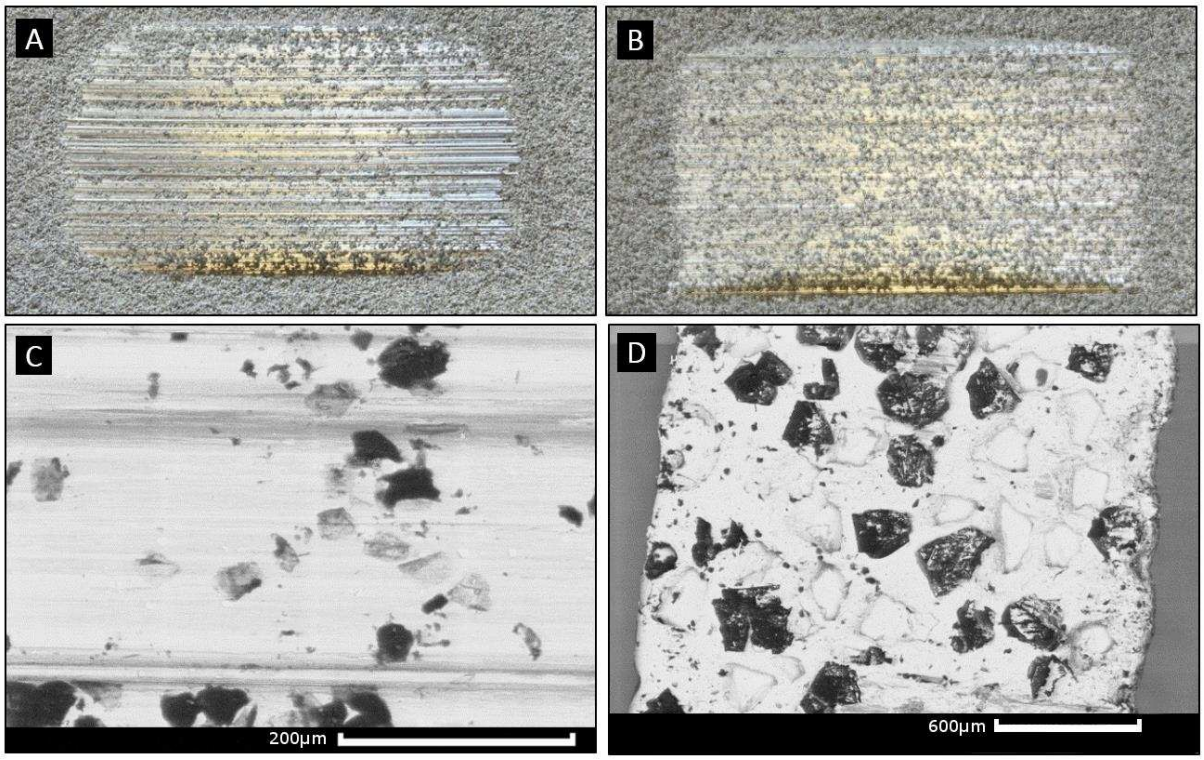

Figure 6 $\begin{matrix} a & b \\ c & d \end{matrix}$ *showing the coating samples from tests 3-8M1 (a) and 4-8L1 (b) and backscattered S.E.M. micrographs of the blade tips which produced them, c & d respectively.*

The force, temperature and blade length results measured during the test show many common features. Initially the measured forces and temperature are low. As the test progresses the tip loses cutting efficiency and the forces and temperature increase with an increasing rate but are still lower than recorded with an untipped blade. At some point the forces and temperature spike after which the same cyclic behaviour described above for untipped blades was observed. This spike is not present in the results for test 4-8L1 (Large grits, tip intact at end) and any change in blade length happens after the spike. This suggests that this spike indicates the breakdown of the tip. The results for test 3-8M1 which show the trend typical from many of the results are shown in figure 7.

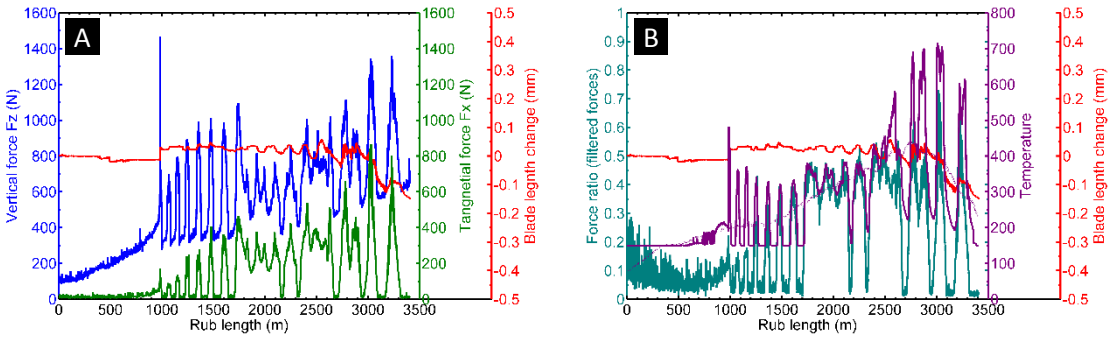

Figure 7(a,b) The force (a), force ratio and temperature (b) results measured during test 3-8M1

Although common trends exist, there is much variation between tests. To allow comparison between different tip types the point at which the tips loose cutting efficiency is used. This is defined as the first point at which the measured normal force exceeds 500N, this value is larger than what is observed for the clean cutting period for any of the blades that showed a definite spike in forces. The results of all the tests performed at 0.02µm/pass are shown in table 3 below. These show that the large grits give a significant advantage over an untipped blade with lower tangential forces and temperatures. It is also clear that friable grits out performed high strength grits at the size tested.

3.2.2 Cr(Al)N coated blades - 0.02µm/pass

The flat Cr(Al)N coated blade from test 6-CF1 appeared worn with a small shear lip present on the trailing edge, as shown in figure 8a. The corresponding coating showed a very small wear scar with a shiny surface which was identified as transfer of Inconel by XRF (2.76% Fe, 12 standard deviations from mean). However the Cr(Al)N coated blade with a 30° chamfered tip (test 7-CC1), shown in figure 8c, was not noticeably worn post-test and it's corresponding coating showed a full length wear scar with a rough dull surface characteristic of clean cutting, these coatings are shown in figure 8(b, d) below.

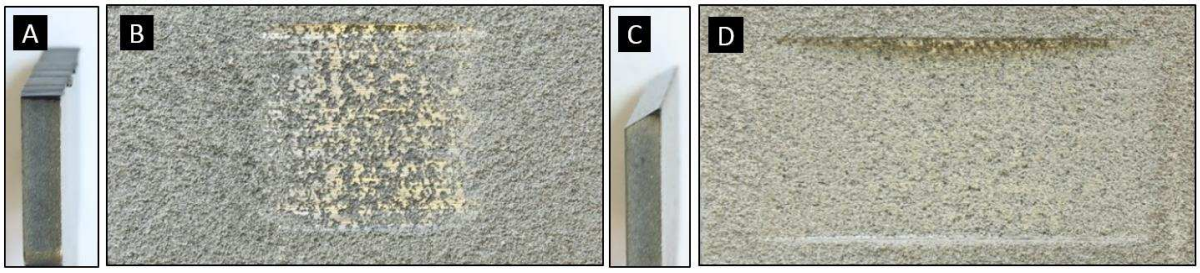

Figure 8 (a-d) Blade and coating samples from test 7-CF1 and 8-CC1 respectively. Blades are 2mm thick, wear tracks are 20mm high.

Force and temperature results, summarised in table 3, show the flat tipped blade reverted to cyclic type behaviour with high coating temperatures almost instantly with blade wear starting very early in the test. Wear debris, collected from this test by affixing carbon S.E.M. stubs to the rig casing, contained long thin chips as shown in figure 9a. These chips are characteristic of chips formed when machining materials with a long elongation to failure[22], this is only a property on Inconel 718 at temperatures exceeding 900°c[23]. The presence of these chips and the large proportion of blade wear indicate that the blade became soft enough to be machined by either the abradable or flakes of Cr(Al)N. Conversely the 30° chamfered blade did not produce temperature in the measuring range of the pyrometer (150°c) and showed forces gradually increasing throughout the test but never

exceeding the 500N limit discussed above. Sectioning of the chamfered blade revealed that the hard coating had been removed from the tip and flank face of the blade near the tip as show in figure 9b.

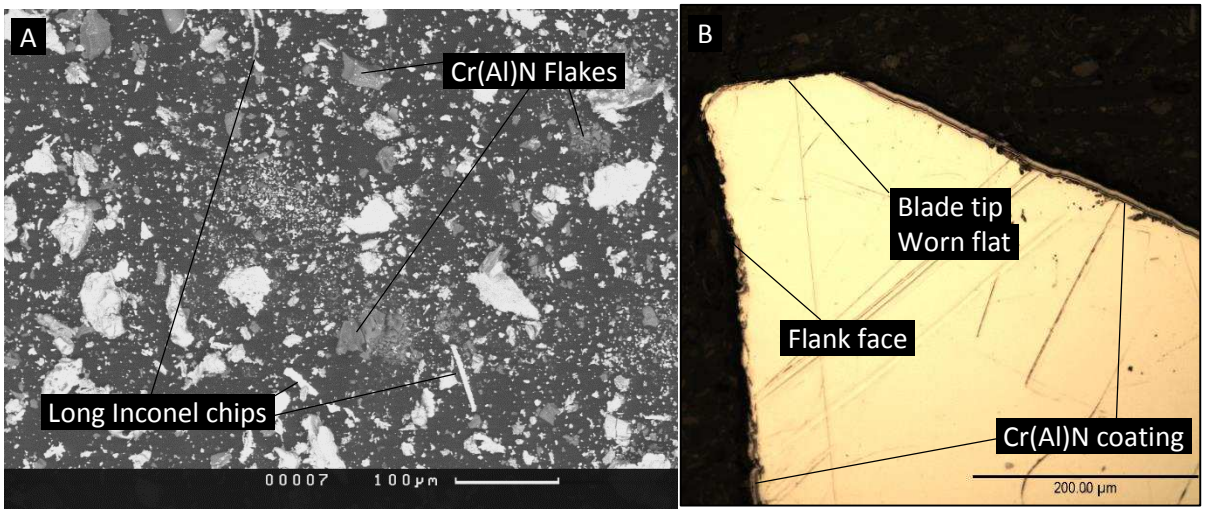

Figure 9 (a, b) showing wear debris collected during test 6-CF1 and a polished cross section of the chamfered blade from test 7-CC1 respectively

Test Number	Rub length at normal force >500N (m)	Maximum normal force (N)	Maximum Tangential Force (N)	Maximum temperature (°C)	Total blade length change (mm)
1-NO1	180	1000	500	890	-0.04
2-8S1	980	1900	800	≥1000	-0.11
3-8M1	980	1500	900	720	-0.15
4-8L1	1690	1000	300	420	-0.01
5-3M1	1390	2300	1100	890	-0.34
6-CF1	110	2500	500	≥1000	-1.24
7-CC1	-	470	90	≤150	-0.01

Table 3 summary of results from primary tests with low incursion rate

3.3 High incursion rate (2µm/pass)

3.3.1 Grit (cBN) tipped blades

After the high incursion rate tests all grit tipped blades appear severely worn at either side with no grits visible, however only the blade tipped with small grits has decreased in length across its entire width. In all blades adhered material has formed lips which overhang both the leading and trailing edge of the blades. Sectioning of blades from tests 10-8M2 and 11-8L2 revealed that the centre of the tip is intact but heavily loaded with coating material. Examples of these blades are shown in figures 10 a and c.

The coating samples showed many similarities between the tests, all of the coatings showed wear scar which was covered in adhered blade material (confirmed in all cases by XRF). All of the wear scars also showed evidence of macro rupture in the centre of the wear track, in tracks produced by medium or large high strength grits (tests: 10-8M2 and 11-8L2) the macro rupture extended out of the expected wear track to the edge of the coating sample as shown in figure 10d.

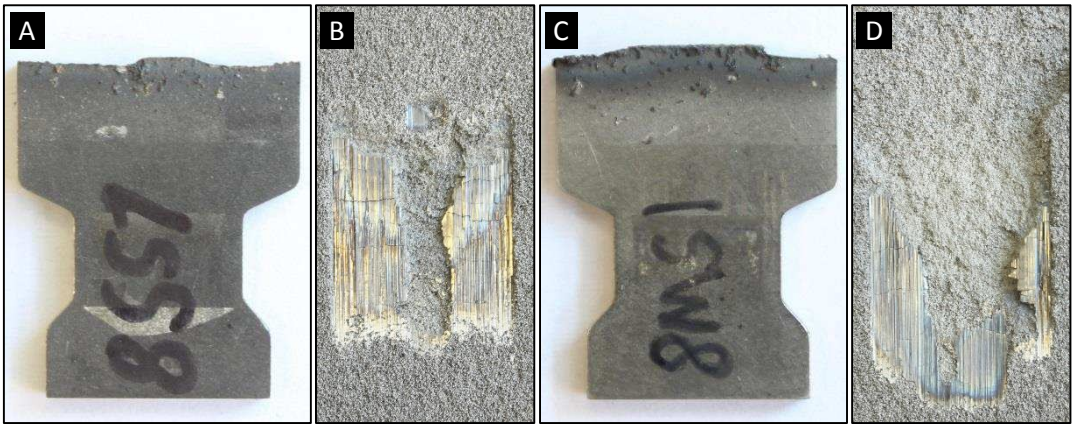

Figure 10 (a-d) showing blade and coating samples from test 9-8S2 and 10-8M2 respectively. Blades and rub tracks are 20mm wide.

Again, the force and temperature results for all grit sizes and types show a common theme. Initially a period of clean cutting, characterised by low forces, force ratio and temperature exists. After this there is a steep rise in forces, temperature and force ratio. This is followed by a decline in normal force towards the end of the test and in the case of the small grit blades a drop in blade length is also seen after the peak normal force. This trend is illustrated in figure 11 below which shows the recorded variables for test 9-8S2. The results of each test performed with an incursion rate of 2µm/pass are summarised in table 4 below. As above the rub length at which the normal force first exceeds 500N is taken as indicative of the time to failure.

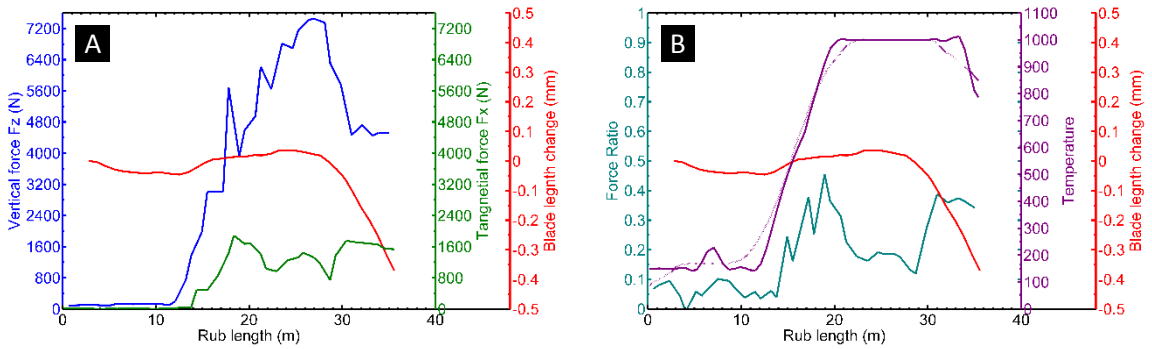

Figure 11 (a, b) showing force (a), force ratio and temperature (b) data collected from test 9-8S2

3.3.2 Cr(AL)N coated blades - 2µm/pass

Both of the Cr(Al)N coated blades were worn heavily after the test and it is assumed that the Cr(Al)N coating has been removed from the blade tip during the test. The coating samples show small wear scars with large areas of thick transfer, the coating which was run against a flat tipped blade also shows slight macro rupture. Both the blade and coating samples are shown in figure 12 below.

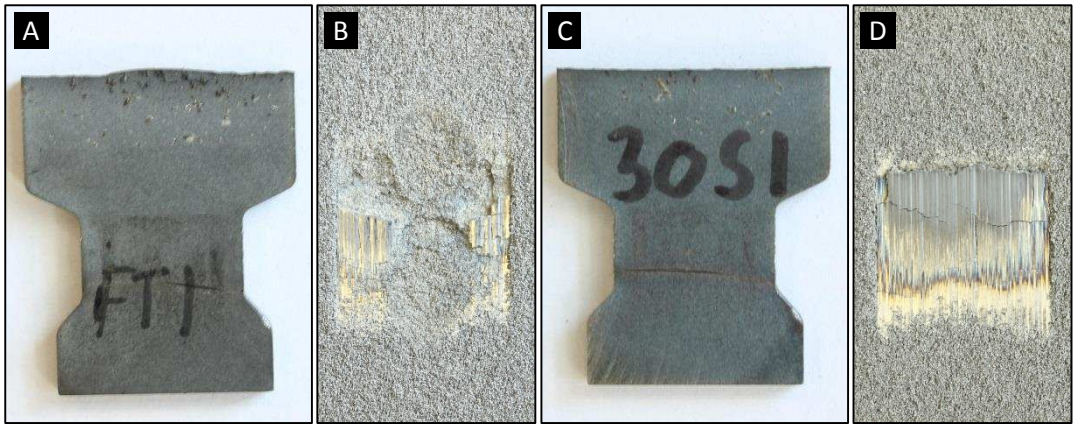

Figure 12 (a-d) showing blade and coating samples from tests 13-CF2 and 14-CC2 respectively. Blades and rub tracks are 20mm wide.

The force and temperature results for the flat tipped blade were similar to the un-tipped blade in both form and magnitude. The chamfered blade produced similar force results to many of the tipped blades with a period of low force which ends just before the first reduction in blade length is detected.

Test Number	Rub length at normal force >500N (m)	Maximum normal force (N)	Maximum Tangential Force (N)	Maximum temperature (°C)	Total blade length change (mm)
8-NO2	0.84	5100	1600	990	-1.12
9-8S2	7.23	7500	1900	≥1000	-0.82
10-8M2	14.89	8400	2400	≥1000	0.01
11-8L2	14.43	8500	2300	620	-0.06
12-3M2	11.66	7800	2300	≥1000	0.01
13-CF2	1.78	5100	1900	970	-1.12
14-CC2	17.12	5200	2100	950	-0.92

Table 4 summary of results from primary tests with high incursion rate

4. Further analysis: Characterising tip behaviour

Many of the blade tips finish tests either completely destroyed or very heavily damaged, often they are loaded with abradable coating material. This process can happen in a number of ways and the resulting blade and coating samples are not adequate to determine the failure mechanism. In order to more fully understand the wear mechanisms that lead up to failure several coating specimens were stepped by face milling[8] in order to rub different parts of the same blade different distances. This method allows snapshots of the state of the blade and coating during different times in the test to be seen. The face milling machine used has an accuracy of 0.3mm, in terms of rub length during the test this leads to an unacceptable error, to counter this rub lengths have been calculated from measurements of the stepped samples that were taken with a micrometre with an accuracy of 0.001mm the error on the relative rub lengths is therefore no more than 1% on the results discussed. An example pair of test specimens is shown in figure 13.

A selection of tests from the initial results which cover the behaviours discussed above have been repeated against stepped coatings. The measured results from the original test against a flat coating are used to target the size of the steps and the total incursion depth of the stepped test to give snapshots at rub lengths leading up to the first spike in force and temperature. During this period in the original test the forces and temperature of the rub change quickly and it is thought that this

relates to a change in the rubbing surfaces. After this period many of the blades show behaviour which is similar to untipped blades. A list of the stepped tests performed is given in table 5 below with their total incursion depths and the rub lengths of each step.

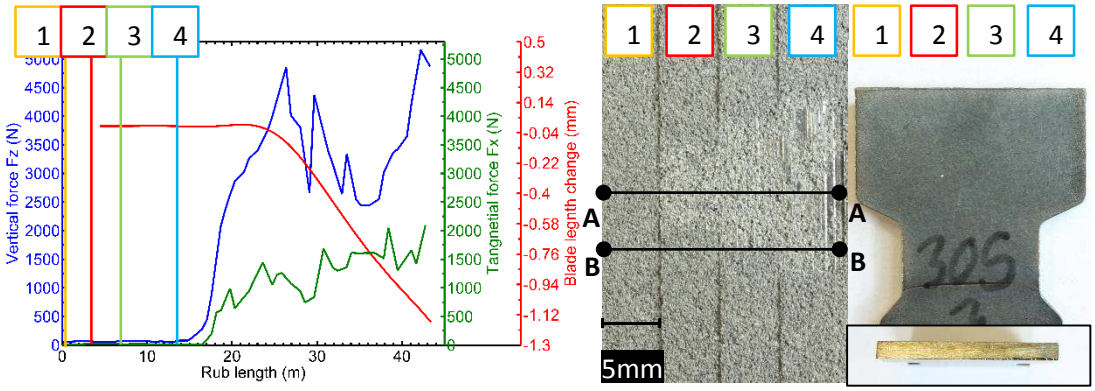

Figure 13 showing the test specimens from test CC2s and the force/ blade length data collected during test 16-CC2 which was performed with the same incursion rate, blade speed and blade type against a flat coating.

Test number	Blade type	Incursion rate (µm/pass)	Incursion depth (µm)	Rub length (m)				
				1	2	3	4	Failure of first test
3M1s	300 medium	0.02	700	57.8	425	881	1680	1390
8S1s	800 small	0.02	550	18.9	247	646	1170	980
8M1s	800 medium	0.02	500	0	66.7	369	1010	980
CF1s	Cr(Al)N Flat	0.02	600	5.20	348	794	1332	110
3M2s	300 medium	2	500	0	0.71	4.02	10.1	11.66
8M2s	800 medium	2	700	1.67	6.07	11.1	16.8	14.89
8L2s	800 large	2	700	1.56	5.64	10.4	16.8	14.43
CF2s	Cr(Al)N Flat	2	600	0.23	3.26	7.80	13.3	1.78
CC2s	Cr(Al)N chamfered	2	600	0.61	2.96	7.39	13.3	17.12

Table 5 summary of secondary tests completed

4.1 Low incursion rate 0.02µm/pass

4.1.1 Grit (cBN) tipped blades

Test 8M1s represents the behaviour seen with small and medium high strength grits at the lower incursion rate (0.02µm/pass). Initially the tip appears well populated with grits that protrude aggressively from the electroplated nickel as shown in figure 14 a. After a relatively small distance many of these grits have been removed leaving only flatter grits (figure 14 b), as the test progresses material from the abradable coating adheres onto these grits eventually bridging between some grits and causing others to fracture, shown in figure 14 c. This process is highly analogous to loading seen on electroplated cBN grinding wheels as described by Gift et. al.[24]. Partial or complete removal of grains of cBN allows the nickel infill to contact directly with the abradable, with the remaining grains becoming increasingly loaded with metal from the abradable, the tip is no longer able to cut efficiently. This process is likely to be self-perpetuating due to softening of the abradable and the infill with higher temperatures, causing more loading, further removal of grits and eventual failure of the tip.

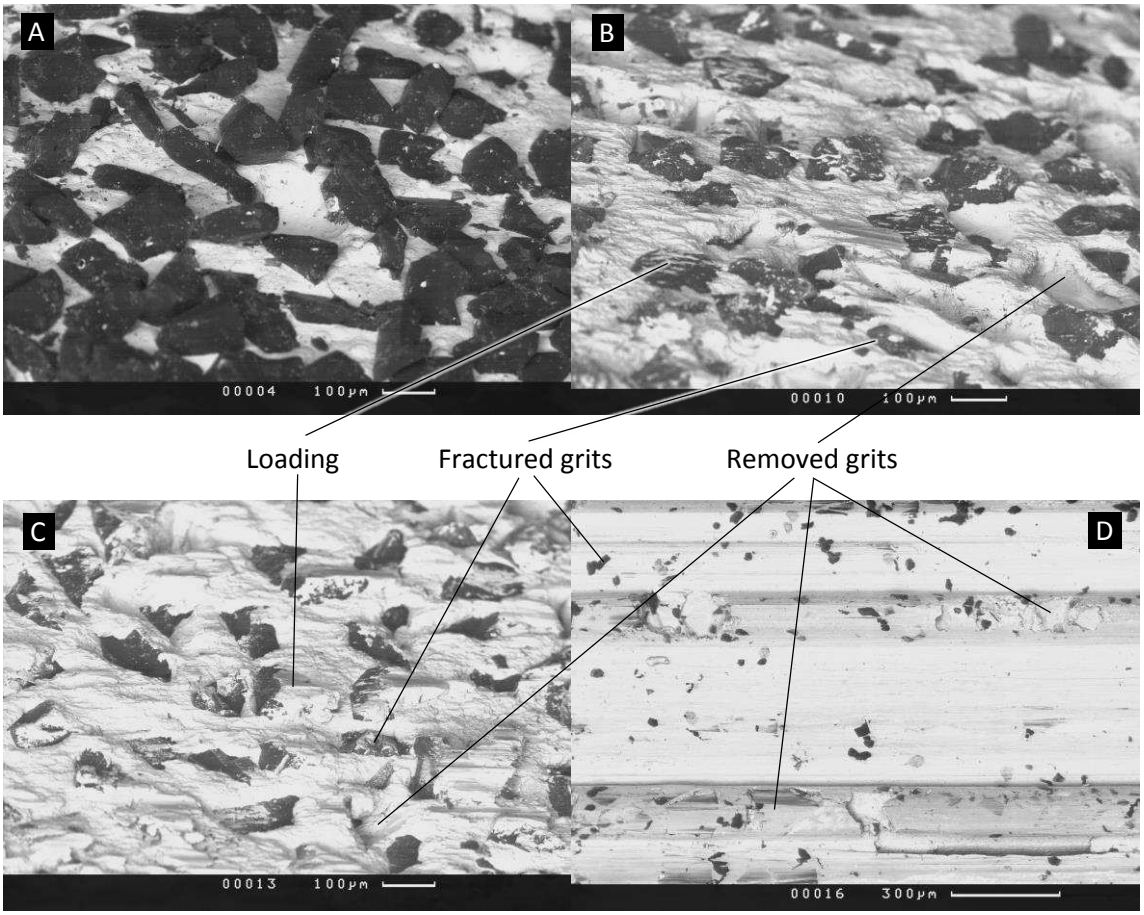

Figure 14 $\begin{matrix} a & b \\ c & d \end{matrix}$ *showing the blade tip of test 8M1s at steps 1 (0 m rub length), 2 (66.7m) and 4 (1010m) and the tip of the blade from test 3-8M1 (3500m)*

Alternative behaviour was observed when the test was repeated with more friable grits, S.E.M. micrographs of the blade tips showed very little pull out of entire grits compared to high strength grits at similar rub lengths. The grits show fractured surfaces which are relatively free from adhered material up to 881m rub length as shown in figure 15 a. This length relates to the plateau in force ratio and temperature as observed above for blades tipped with friable grits. The plateau and extended blade life is thus attributed to the semi stable mechanism of grit loading and breaking on a small scale. The section of blade which was rubbed for 1680m is shown in figure 15 b and represents the blade as it is just before the first spike in temperature and force. Many of the grits have fractured below the height of the electroplated nickel infill; at this point smears in the infill material extend around half way across the blade from the front edge. Behind these smears remaining cBN grains are coated on the leading side with metal from the abradable lining (identified BY E.D.S.) which is globular in appearance.

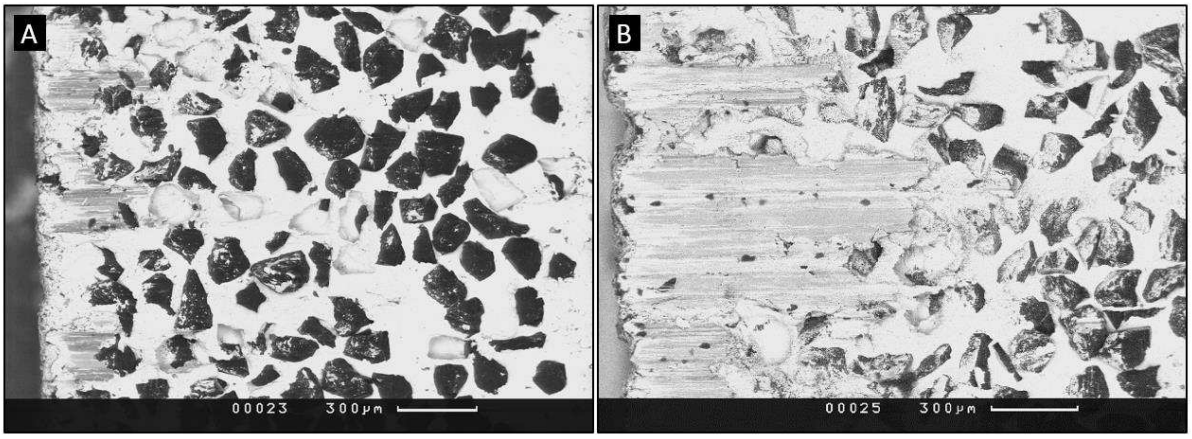

Figure 15 (a, b) showing the blade tip from test 3M1s at step 3 (881m rub length) showing broken grits and step 4 (1680m rub length) showing smears of metal from the abradable material respectively

Coating samples for all stepped tests performed with grit tipped blades at the lower incursion rate appeared to be cleanly cut indicating that until failure the grits are able to work effectively. The only exception to this was the test with small grits (8S1s) which showed a layer of metal that could not be identified as Inconel 718 transfer on step 4, this layer was not present on the coating after the full depth rub (test 2-8S1).

Previous work[14] on this coating has shown that it can compact rather than cut under some conditions. In these conditions the porosity of the coating is reduced near the rubbing surface resulting in a hard layer consisting of only metal and bentonite phases. To determine if compaction had occurred the coating samples were sectioned along line A-A in figure 13 allowing micrographs to be taken from under the centre of the rub track. Four micrographs were taken for each step of the coating, these were then passed through a threshold filter using an automatic threshold selected to minimise interclass variance[19]. This step is considered more accurate than keeping the same threshold value for each photograph due to differences in reflectivity of the samples and ambient lighting present during image acquisition. The resulting images were then analysed to give the fraction of lighter material (metal phase) at each of 10 different levels, this was compared to a similar set of 37 images taken of the 'as sprayed' condition to account for variations due to the spraying process. Examples of an image from the control set and of a compacted coating are shown in figure 16. This approach allows compaction to be quantified in both severity and depth. Using this technique compaction was not found in any of the coating samples from these tests indicating that up to the failure of the tip the abradable has been able to dislocate effectively.

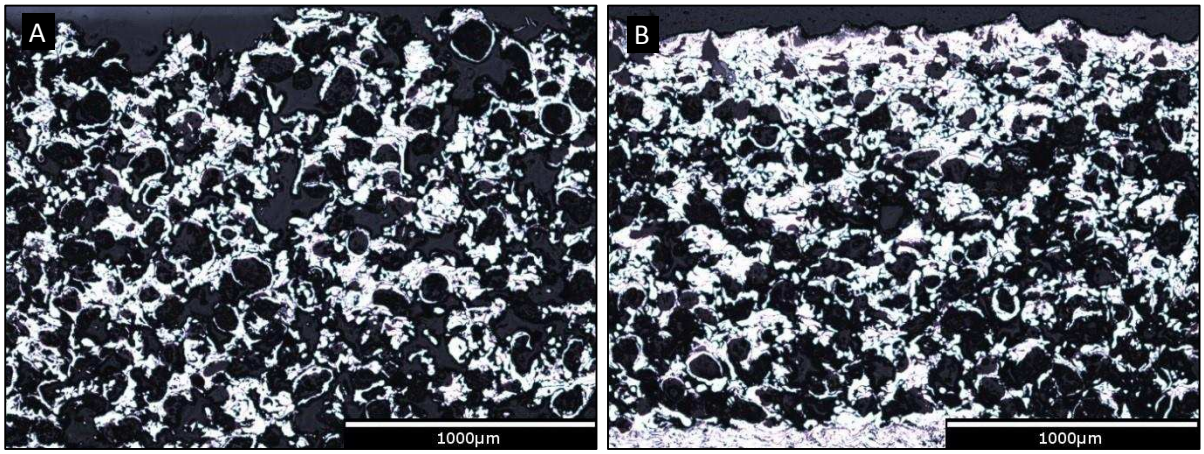

Figure 16(a, b) example micrographs of sections of the abradable coating in the as sprayed condition and after the deepest incurring step in test 8L2s respectively

4.1.2 Cr(Al)N coated blades 0.02µm/pass

At the low incursion rate the coated blades behaved very differently depending on the tip morphology, the chamfered blades cut the coating cleanly with the lowest recorded forces and temperatures of any test and no blade damage whereas the flat blades performed worse than any of the other blades in terms of blade wear. For this reason only the test with the flat blade was repeated against a stepped coating.

The back scattered electron image of the tip of the flat blade is shown in figure 17 step one shows smears of material on the flank face of the blade. Profilometry, shown in figure 17, shows that these smears of material are higher than the surrounding coated blade material indicating that material has adhered onto the Cr(Al)N coating from the abradable. Beyond the first step x-ray florescence shows the Cr(Al)N coating has been removed and the composition is as expected for plain Inconel 718.

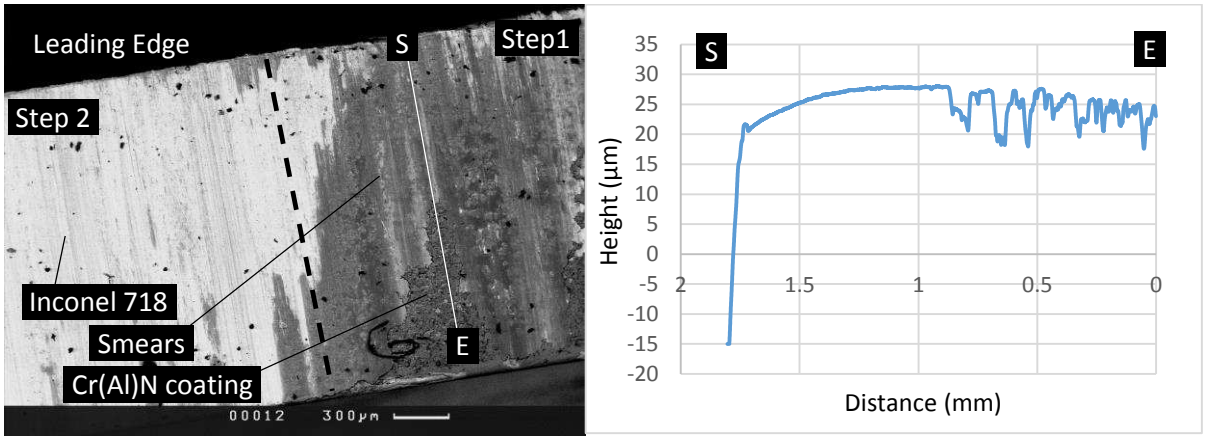

Figure 17 back scattered electron image of the blade from test CF1s showing areas of blade which were rubbed against step 1 (5.2m rub length) and step 2 (348m rub length) right and left respectively and profilometry measurements from the imaged blade.

The abradable coating sample appeared cleanly cut for all steps apart from step 2 which showed a shiny layer of material which when analysed with XRF had a Cr/Ni ratio of 0.476, 55 standard deviations above the mean value of 0.07 for un-worn abradable samples and an iron content within the expected range for unworn abradable samples. Thus this shiny layer has been identified as transfer of the Cr(Al)N coating on to the abradable.

Previous tribological experiments with Cr(Al)N coatings have also observed metal adhering directly onto the coating[25], [26], and further testing has shown that these coatings can lose adherence to the substrate resulting in the coating flaking off when rubbed at moderately high temperatures[26]. This mechanism is considered likely and is supported by the presence of plate like structures with a composition of mostly chromium and aluminium in the wear debris from these tests as shown in figure 9a.

This mechanism accounts for the drop in performance of the flat blade compared to an uncoated blade, as the coated blade is heated quickly due to its high friction coefficient on the flank face and the presence of hard flakes of Cr(Al)N as third bodies in the rub could cause increased blade wear later in the test. As the Cr(Al)N family of coatings are the only commonly available hard coatings

which will not oxidise in the compressor (T≈800°c) [27] hard coatings alone are not a viable solution to prevent blade damage.

4.2 High incursion rate (2µm/pass)

4.2.1 Grit (cBN) tipped blades

At the higher incursion rate the grit tipped blades performed in a similar way. Every blade loaded quickly, as described above, with adhered metal from the abradable lining. The rate of loading seems dependant on the size of the grit for high strength grits with larger grits taking longer to fully load. The medium sized friable grits acted in a similar way to small high strength grits, becoming loaded very early in the test. The adhered material loads directly onto the grits and bridges gaps between them as shown in figure 18 a. During this process some grits are also removed from the leading edge of the blades. The blades become fully loaded early in the test (rub length=4-6m) and before the spike in forces associated with failure as discussed above and listed in table 4 (typical rub length 11-17m).

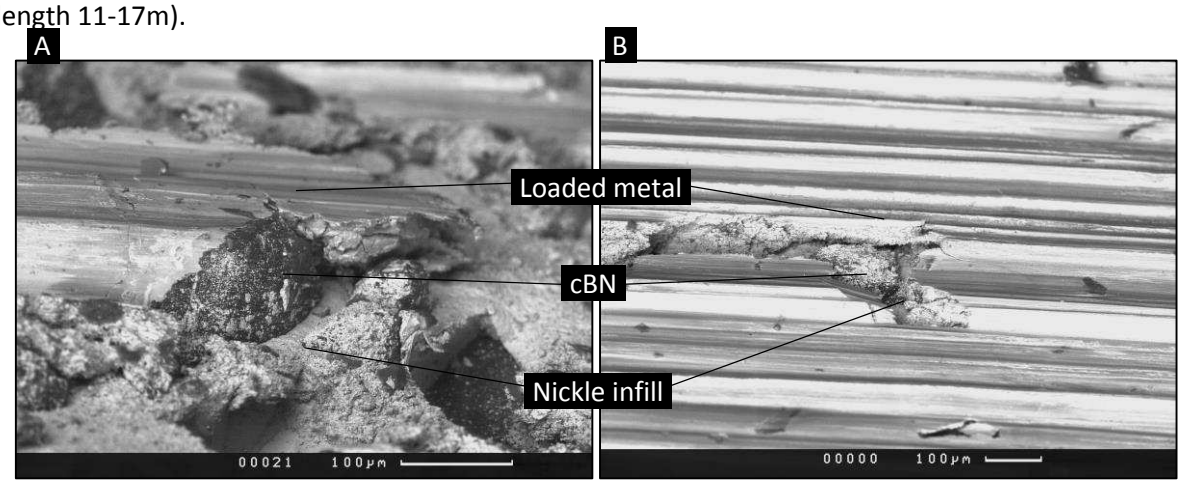

Figure 18 (a, b) showing loading on to grains on cBN on the tip of the blade from test 8L2s step 2 (5.64m rub length) and test 3M2s step 3 (4.02m rub length) respectively

As above the coating samples from these tests were sectioned, imaged and analysed to see if the coating had become compacted during the test. The results of this analysis show there is no compaction of the coating in the steps of the coating which had not been rubbed far enough to fully load the blade tips. The coating becomes more severely compacted as the incursion depth increases after the tip has become loaded. Further sections were taken at the edge of the deepest rub, line B in figure 19, at a point at which the coating had been cut to the same depth as the centre of the shortest rub. Analysis of these sections shows severe but shallow compaction indicating that compaction of the coating is not simply a consequence of incursion depth, or rub length and is instead due to loss of cutting efficiency of the tip. The extensive macro rupture observed in the coating samples from earlier tests is then due to removal of the entire compacted layer and is distinct from failure mechanisms such as spalling caused by contact fatigue. The result of this analysis is the same for each of the coating samples from the high incursion rate, stepped coating tests the full result from test 8L2s is shown below in figure 20 as an example.

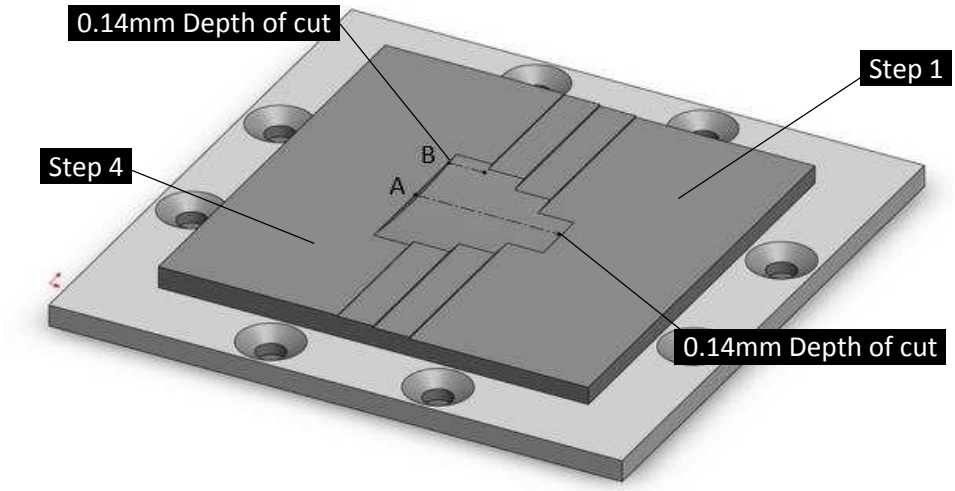

Figure 19 showing the coating sections taken for compaction analysis

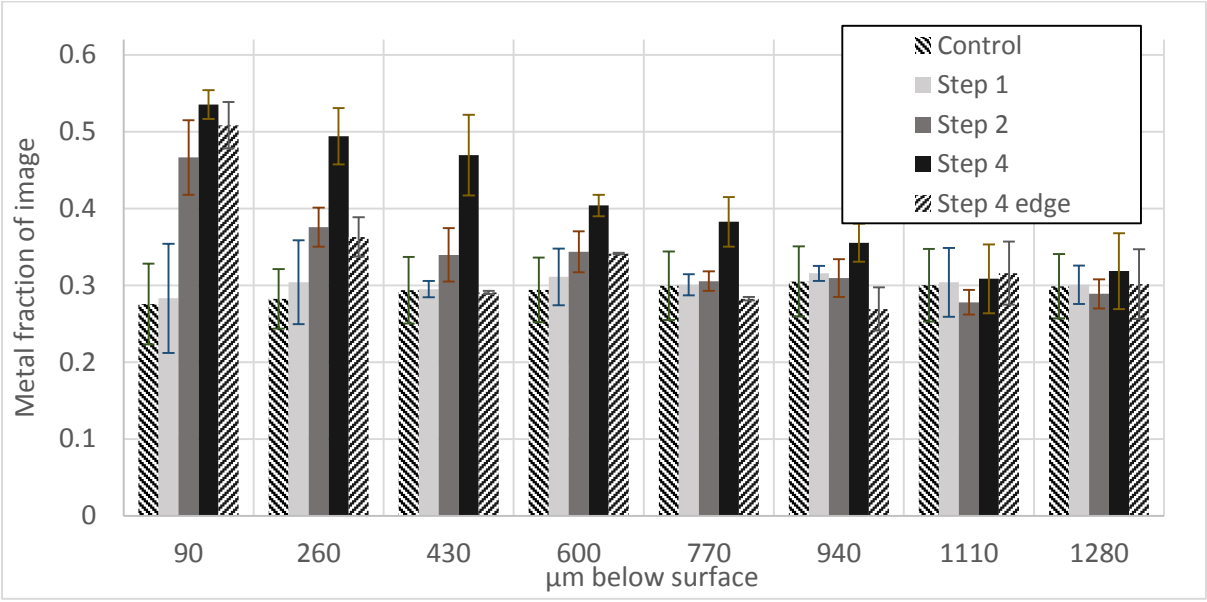

Figure 20 showing results of image analysis on the section images taken of the coating sample from test 8L2s. Error bars indicate one standard deviation and are shown for the control set, step 2 and step 4 only.

4.2.2 Cr(Al)N coated blades – 2µm/pass

The flat Cr(Al)N coated blades showed a similar mechanism to that discussed above for low incursion rate tests; smears of adhered material are visible on the blade at the start of the test and wear debris analysis again showing plate like structures of chromium and aluminium similar to those shown in figure 9 a. In this case melt wear of the blade followed as evidenced by the presence of small spheres of metal with a composition between that of the blade and the metal phase of the abradable lining in the wear debris. It is unlikely that these spheres were created by contact fatigue due to the length of the test (5s, 1000 cycles) and their abundance in the debris. Long chips of Inconel, seen for low incursion rate tests, were not observed in the wear debris.

The stepped chamfered blade initially showed cracking of the sharp tip, followed by adhesion of chips to the rake face with subsequent removal of the coating again in large flakes, indicating loss of adhesion to the substrate and interlayer cracking of the coating with a mechanism similar to that of crater wear in high speed machining[28], followed by removal of the cratered section of tip. As this

process continues the blade gains a flank face and frictional heating and three body abrasion takes over as the dominant wear mechanism as for flat blades. Micrographs of the blade indicating this process are shown in figure 21 below.

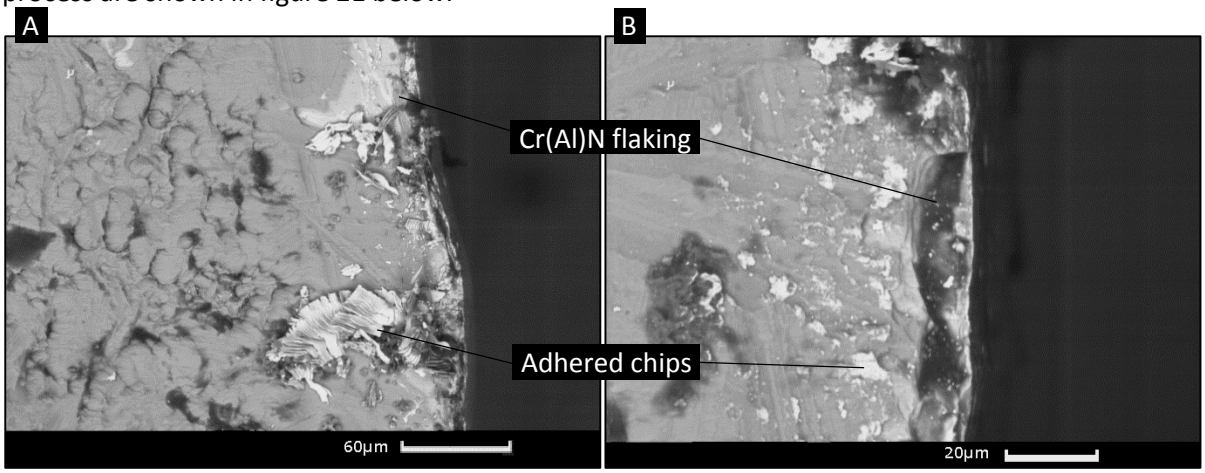

Figure 21 (a, b) showing steps 2 (left, 2.96m rub length) and 3 (right, 7.39m rub length) of the blade sample from test CC2s showing chip adhesion and loss of flakes of coating.

5. Conclusions

The purpose of this experimental study was to evaluate tipping and coating methods for the next generation of compressor blades. To this end tests were performed on a scaled test rig with a blade tip speed of 200m/s and incursion rates of 0.02µm/pass and 2µm/pass. The major conclusions are summarized as follows:

1. Adding grits to the top of blades produced a period of clean cutting with low forces and temperatures at the start of the test. However at both incursion rates these tips caused more catastrophic failure mechanisms and produced much higher forces than seen in an untipped blade if they became loaded.
2. At a low incursion rate (0.02µ/pass) blades tipped with high strength grits showed pull out of entire grits at the start of the tests followed by loading directly on to the grit. Friable grits showed similar behaviour with the addition of a semi stable loading/ grit breaking period, which extended the life of the tip. Larger grits were able to cut the abradable lining efficiently for the entire test with low forces and temperatures measured.
3. At the high incursion rate (2µ/pass) all of the grit tips became loaded with material from the abradable lining adhering directly onto the cBN grits. The time to failure appeared to the dependant on the size of the grit with the exception of the blade tipped with friable grits which loaded more quickly than expected. This loading resulted in a loss of cutting efficiency and caused compaction in the coating leading to extremely high rubbing forces and the eventual failure of the tip in cases with small or friable grits or macro rupture of the abradable lining.
4. Addition of a multi-layer Cr(Al)N coating was detrimental to performance of the blade unless a chamfer was also added to the blade tip. Blades with this coating and no chamfer produced the largest loss of blade length observed for any blade in both the high and low incursion rate tests. This is due to hard particles of the Cr(Al)N coating being present in the rub after it failed early in the test because of poor high temperature tribological properties.
5. Cr(Al)N coated chamfered blades produced the longest time to failure in the high incursion rate test and the best cutting performance (with no failure) in the low incursion rate tests. Failure of the chamfered blades appeared to be due to wear on the rake face of the blade

caused by adhesion of chips. It is not clear weather their performance is due to the Cr(Al)N coating or the tip morphology, this will be the subject of future research.

Tests at lower speeds have shown even more severe compaction and macro rupture of the abradable coating, future work by this group will investigate whether higher speeds alleviate the compaction issue that has been observed here. ~~Platinum~~ Alternative coatings have also been tested on grit tipped blades to delay adhesion on to grits with a modest increase in blade life observed for the high incursion rate rubs. Should a coating prove successful, this will then require further investigation within the batch-to-batch variation of nominally similar abradable materials.~~, inherent d~~Due to inherent randomness in the thermal spray ~~the~~ process through which they are manufactured.

References

[1] N. Fois, M. Watson, J. Stringer, and M. Marshall, "An investigation of the relationship between wear and contact force for abradable materials," *Proc. Inst. Mech. Eng. Part J J. Eng. Tribol.*, Jul. 2014.

[2] N. Fois, J. Stringer, and M. B. Marshall, "Adhesive transfer in aero-engine abradable linings contact," *Wear*, vol. 304, no. 1–2, pp. 202–210, Jul. 2013.

[3] D. Sporer, S. Wilson, and S. M. Ag, "Current and Next-Generation Titanium Blade Compatible Compressor Abradable Coatings," in *Thermal spray 2012: Proceedings from the international thermal spray conference and exposition*, 2012, pp. 143–148.

[4] H. I. Faraoun, T. Grosdidier, J.-L. Seichepine, D. Goran, H. Aourag, C. Coddet, J. Zwick, and N. Hopkins, "Improvement of thermally sprayed abradable coating by microstructure control," *Surf. Coatings Technol.*, vol. 201, no. 6, pp. 2303–2312, Dec. 2006.

[5] M. Clegg and M. Mehta, "NiCrAl/bentonite thermal spray powder for high temperature abradable seals," *Surf. Coatings Technol.*, vol. 34, pp. 69–77, 1988.

[6] X. Ma and A. Matthews, "Evaluation of abradable seal coating mechanical properties," *Wear*, vol. 267, no. 9–10, pp. 1501–1510, Sep. 2009.

[7] R. E. Johnston and W. J. Evans, "Freestanding abradable coating manufacture and tensile test development," *Surf. Coatings Technol.*, vol. 202, no. 4–7, pp. 725–729, Dec. 2007.

[8] R. E. Johnston, "Mechanical characterisation of AlSi-hBN, NiCrAl-Bentonite, and NiCrAl-Bentonite-hBN freestanding abradable coatings," *Surf. Coatings Technol.*, vol. 205, no. 10, pp. 3268–3273, Feb. 2011.

[9] Y. Maozhong, H. Baiyun, and H. Jiawen, "Erosion wear behaviour and model of abradable seal coating," *Wear*, vol. 252, no. 1–2, pp. 9–15, Jan. 2002.

[10] X. Ma and A. Matthews, "Investigation of abradable seal coating performance using scratch testing," *Surf. Coatings Technol.*, vol. 202, no. 4–7, pp. 1214–1220, Dec. 2007.

[11] H. Wang, "Criteria for analysis of abradable coatings," *Surf. Coatings Technol.*, vol. 79, pp. 71–75, 1996.

[12] H. I. Faraoun, J. L. Seichepine, C. Coddet, H. Aourag, J. Zwick, N. Hopkins, D. Sporer, and M. Hertter, “Modelling route for abradable coatings,” *Surf. Coatings Technol.*, vol. 200, no. 22–23, pp. 6578–6582, Jun. 2006.

[13] M. Huang and Y. Li, “X-ray tomography image-based reconstruction of microstructural finite element mesh models for heterogeneous materials,” *Comput. Mater. Sci.*, vol. 67, pp. 63–72, 2013.

[14] T. a. Taylor, B. W. Thompson, and W. Aton, “High speed rub wear mechanism in IN-718 vs. NiCrAl–Bentonite,” *Surf. Coatings Technol.*, vol. 202, no. 4–7, pp. 698–703, Dec. 2007.

[15] C. Padova, J. Barton, M. G. Dunn, S. Manwaring, G. Young, M. Adams, and M. Adams, “Development of an Experimental Capability to Produce Controlled Blade Tip/Shroud Rubs at Engine Speed,” *J. Turbomach.*, vol. 127, no. 4, p. 726, 2005.

[16] C. Padova, M. G. Dunn, J. Barton, K. Turner, A. Turner, and D. DiTommaso, “Casing Treatment and Blade-Tip Configuration Effects on Controlled Gas Turbine Blade Tip/Shroud Rubs at Engine Conditions,” *J. Turbomach.*, vol. 133, no. 1, p. 011016, 2011.

[17] Sultzer Metco, “Material Product Data Sheet Nickel Chromium Aluminum / Bentonite Abradable Powders.” pp. 3–6, 2012.

[18] S. Deshpande, a Kulkarni, S. Sampath, and H. Herman, “Application of image analysis for characterization of porosity in thermal spray coatings and correlation with small angle neutron scattering,” *Surf. Coatings Technol.*, vol. 187, no. 1, pp. 6–16, Oct. 2004.

[19] N. Otsu, “A threshold selection method from gray-level histograms,” *Automatica*, vol. C, no. 1, pp. 62–66, 1975.

[20] J. Stringer and M. B. Marshall, “High speed wear testing of an abradable coating,” *Wear*, vol. 294–295, pp. 257–263, Jul. 2012.

[21] D. Sporer, S. Wilson, P. Leader, and M. Giannozzi, “On the potential of metal and ceramic based abardables in turbine seal applications,” in *Proceedings of the thirty-sixth turbomachinery symposium*, 2007, pp. 79–86.

[22] W. Grzesik, *Advanced Machining Processes of Metallic Materials*. Elsevier, 2008.

[23] Special metals, *INCONEL alloy 718 Data Sheet*. .

[24] F. C. Gift, W. Z. Misiolek, and E. Force, “Mechanics of Loading for Electroplated Cubic Boron Nitride (CBN) Wheels During Grinding of a Nickel-Based Superalloy in Water-Based Lubricating Fluids,” *J. Tribol.*, vol. 126, no. 4, p. 795, 2004.

[25] L. Wang, X. Nie, J. Housden, E. Spain, J. C. Jiang, E. I. Meletis, a. Leyland, and a. Matthews, “Material transfer phenomena and failure mechanisms of a nanostructured Cr–Al–N coating in laboratory wear tests and an industrial punch tool application,” *Surf. Coatings Technol.*, vol. 203, no. 5–7, pp. 816–821, Dec. 2008.

[26] T. Polcar and A. Cavaleiro, “High-temperature tribological properties of CrAlN, CrAlSiN and AlCrSiN coatings,” *Surf. Coatings Technol.*, vol. 206, no. 6, pp. 1244–1251, Dec. 2011.

[27] Y. Chim, X. Ding, X. Zeng, and S. Zhang, “Oxidation resistance of TiN, CrN, TiAlN and CrAlN coatings deposited by lateral rotating cathode arc,” *Thin Solid Films*, 2009.

[28] C. Y. H. Lim, S. C. Lim, and K. S. Lee, “Crater wear mechanisms of TiN coated high speed steel tools,” *Surf. Eng.*, vol. 16, no. 3, pp. 253–256, 2000.